

- [6] T. J. Crevier, B. K. Bennett, J. D. Soper, J. A. Bowman, A. Dehestani, D. A. Hrovat, S. Lovell, W. Kaminsky, J. M. Mayer, *J. Am. Chem. Soc.* **2001**, *123*, 1059–1071.
- [7] From a complete search of the Cambridge Structural Database, the data include all parent imido transition metal complexes up to June of 2001.
- [8] a) W. A. Herrmann, A. W. Stumpf, T. Priermeier, S. Bogdanovic, V. Dufaud, J.-M. Basset, *Angew. Chem.* **1996**, *108*, 2978–2980; *Angew. Chem. Int. Ed. Engl.* **1996**, *35*, 2803–2805; b) W. A. Herrmann, S. Bogdanovic, R. Poli, T. Priermeier, *J. Am. Chem. Soc.* **1994**, *116*, 4989–4990; c) J. Chatt, R. Choukroun, J. R. Dilworth, J. R. Hyde, P. Vella, J. Zubieta, *Trans. Met. Chem.* **1979**, *4*, 59–63; d) J. Chatt, J. R. Dilworth, *J. Chem. Soc. Chem. Commun.* **1975**, 983–984; e) C. C. Cummins, R. R. Shrock, W. M. Davis, *Inorg. Chem.* **1994**, *33*, 1448–1457.
- [9] a) J. R. Dilworth, J. S. Lewis, J. R. Miller, Y. Zheng, *J. Chem. Soc. Dalton Trans.* **1995**, 1357–1361; b) J. R. Dilworth, P. L. Dahlstrom, J. R. Hyde, J. Zubieta, *Inorg. Chim. Acta.* **1983**, *71*, 21–28; c) J. R. Dilworth, R. Henderson, P. L. Dahlstrom, J. Hutchinson, J. Zubieta, *Cryst. Struct. Commun.* **1982**, *11*, 1135–1139.
- [10] A. Haug, J. Strähle, *Z. Anorg. Allg. Chem.* **1998**, *624*, 1746–1750.
- [11]  $[\text{Os}^{\text{III}}(\text{Tp})(\text{Cl})_2(\text{NH}_3)]$  and  $[\text{Os}^{\text{VI}}(\text{Tp})(\text{Cl})_2(\text{N})]$  were previously isolated and characterized, reference [1c].
- [12] Elemental analysis calcd (%) for **7A**Cl:  $\text{OsC}_{17}\text{H}_{17}\text{N}_4\text{SOCl}_3 \cdot (\text{H}_2\text{O}$  and  $\text{Me}_2\text{SO})$ : C 31.78, H 3.51, N 7.80; found: C 31.95, H 3.64, N 8.12. **7B**PF<sub>6</sub> elemental analysis calcd (%) for  $\text{OsC}_{17}\text{H}_{17}\text{N}_4\text{SOCl}_2\text{PF}_6$ : C 27.91, H 2.34, N 7.66; found: C 28.23, H 2.52, N 7.87.
- [13] Crystal data:  $P\bar{1}$ , triclinic,  $a = 8.9405(3)$ ,  $b = 10.7563(3)$ ,  $c = 13.8861(4)$  Å,  $\alpha = 109.820(1)^\circ$ ,  $\beta = 103.443(1)^\circ$ ,  $\gamma = 95.231(1)^\circ$ ,  $V = 1217.33(6)$  Å<sup>3</sup>,  $Z = 2$ . Final  $R_1 = 0.033$  and  $wR_2 = 0.035$  using 10537 reflections and 290 parameters. Crystallographic data (excluding structure factors) for the structure reported in this paper have been deposited with the Cambridge Crystallographic Data Centre as supplementary publication no. CCDC-163001 for **7A**Cl. Copies of the data can be obtained free of charge on application to CCDC, 12 Union Road, Cambridge CB21EZ, UK (fax: (+44)1223-336-033; e-mail: deposit@ccdc.cam.ac.uk).
- [14] a) B. B. Snider, *Chem. Rev.* **1996**, *96*, 339–363; b) K. L. Davis, E. Martin, I. V. Turko, F. Murad, *Annu. Rev. Pharmacol. Toxicol.* **2001**, *41*, 203–236; c) F. Murad, *Recent Prog. Horm. Res.* **1998**, *53*, 43–60.
- [15] D. S. Williams, G. M. Coia, T. J. Meyer, *Inorg. Chem.* **1995**, *34*, 586–592.
- [16] IR data for **10**PF<sub>6</sub> and **11**PF<sub>6</sub>: **10**PF<sub>6</sub>:  $\nu(\text{N}-\text{H})$  3187;  $\nu(\text{tpy})$  1458 (vs), 1449 (vs), and 1435 (vs);  $\nu(\text{NN})$  1236 and for **11**PF<sub>6</sub>:  $\nu(\text{N}-\text{H})$  3200;  $\nu(\text{tpy})$  1481 (vs), 1449 (vs), and 1349 (vs);  $\nu(\text{NO})$  1173.
- [17] **10**PF<sub>6</sub>: elemental analysis calcd (%) for  $\text{OsC}_{23}\text{H}_{20}\text{N}_4\text{Cl}_2\text{OPF}_6 \cdot \text{CH}_3\text{CN}$ : C 36.82, H 2.84, N 8.59; found: C 37.14, H 3.04, N 8.75. **11**PF<sub>6</sub>: elemental analysis calcd (%) for  $\text{OsC}_{27}\text{H}_{22}\text{N}_5\text{Cl}_2\text{PF}_6$ : C 39.42, H 2.70, N 8.51; found: C 39.63, H 2.86, N 8.69.

## Chiral Recognition of *O*-Phosphoserine by Mass Spectrometry\*\*

Giovanna Fago, Antonello Filippi, Anna Giardini, Aldo Laganà, Alessandra Paladini, and Maurizio Speranza\*

Reversible protein phosphorylation is involved in a multitude of regulatory mechanisms for the control of intracellular protein functionality.<sup>[1–4]</sup> Serine, threonine, tyrosine, and a number of other amino acid residues can be modified by the attachment of a phosphate group. The exact site of the modification has to be determined to elucidate the physiological impact of this event. This can be a very difficult task since only a small fraction of a given protein may be phosphorylated and phosphorylation may occur at multiple sites, thus giving rise to various phosphorylated forms. Although sensitive analytical methods are available for the detection and quantification of phosphorylation sites,<sup>[5–9]</sup> there is still a great need for further improvements, especially in view of the fact that both *O*-phosphoserine and -threonine cannot be unambiguously assigned by Edman sequencing.<sup>[10]</sup>

In recent years, tandem mass spectrometry (MS<sup>n</sup>) has gained wide recognition as a powerful tool for peptide sequencing and for the identification of modified amino acids within the sequence tag.<sup>[11]</sup> This capability has encouraged the exploration of a mass spectrometric methodology for gas-phase discrimination of chiral analytes ( $A_R$  and  $A_S$ ) through the measurement of the stability<sup>[12–14]</sup> and the reactivity<sup>[12, 15]</sup> of the diastereomeric complexes formed with a chiral reference molecule (ref). The kinetic method proved particularly useful for this task and was exploited by the research groups of Cooks,<sup>[13, 14, 16]</sup> Tao,<sup>[13, 14]</sup> and others.<sup>[17]</sup> The method is based on the collisionally induced dissociation (CID) of the diastereomeric cluster ions  $[\text{M} \cdot (\text{ref})_2 \cdot A_R]^+$  and  $[\text{M} \cdot (\text{ref})_2 \cdot A_S]^+$  ( $\text{M} = \text{H}$  or metal; Figure 1). It is convenient to define the cluster ions as “homo” when the analyte and reference have the same configuration, and “hetero” in the opposite case.

According to the foundations of the kinetic method used by Cooks and co-workers,<sup>[13, 16]</sup> CID of  $[\text{M} \cdot (\text{ref})_2 \cdot A_R]^+$  and  $[\text{M} \cdot (\text{ref})_2 \cdot A_S]^+$  may produce different fragmentation patterns that reflect the stability of  $[\text{M} \cdot \text{ref} \cdot A_R]^+$  (and  $[\text{M} \cdot \text{ref} \cdot A_S]^+$ ) relative to  $[\text{M} \cdot (\text{ref})_2]^+$  ( $\Delta G_R$  and  $\Delta G_S$ , respectively).

[\*] Prof. M. Speranza, Dr. A. Filippi  
Facoltà di Farmacia, Dipartimento No. 64 (SCTSBA)  
Università degli Studi di Roma “La Sapienza”  
P.le A. Moro 5, 00185, Roma (Italy)  
Fax: (+39) 6-49913602  
E-mail: speranza@axrma.uniroma1.it

Dr. G. Fago, Prof. A. Giardini, Prof. A. Laganà, Dr. A. Paladini  
Dipartimento di Chimica  
Università degli Studi di Roma “La Sapienza”  
P.le A. Moro 5, 00185 Roma (Italy)  
Prof. A. Giardini  
CNR - Istituto Materiali Speciali  
85050 Tito Scalo (Pz) (Italy)

[\*\*] This work was supported by the Ministero della Università e della Ricerca Scientifica e Tecnologica (MURST) and the Consiglio Nazionale delle Ricerche (CNR). The authors express their gratitude to F. Angelelli for technical assistance.

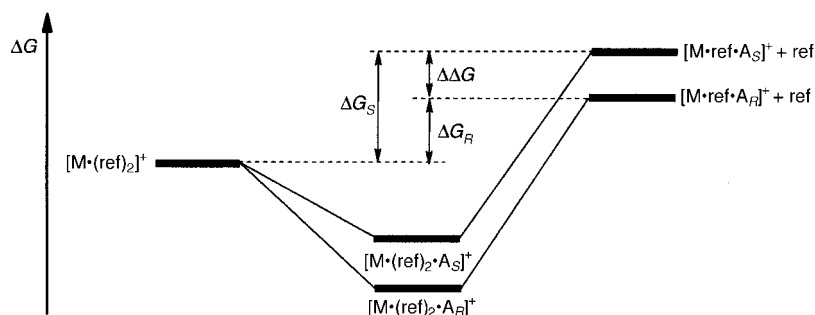


Figure 1. Free-energy diagram for the dissociation of trimeric cluster ions.

Measurement of the ratio of the “homo” versus “hetero” ion abundance ratios provides the chiral selectivity  $R_{\text{chiral}}$  [Eq. (1)]

$$R_{\text{chiral}} = \frac{R_{\text{homo}}}{R_{\text{hetero}}} = \frac{[\text{M} \cdot \text{ref} \cdot \text{A}_S]^+ / [\text{M} \cdot (\text{ref})_2]^+}{[\text{M} \cdot \text{ref} \cdot \text{A}_R]^+ / [\text{M} \cdot (\text{ref})_2]^+} \quad (1)$$

if the *S* enantiomer of the reference is employed, and  $R'_{\text{chiral}}$  [Eq. (2)] if the *R* enantiomer of the reference is employed. The

$$R'_{\text{chiral}} = \frac{R'_{\text{homo}}}{R'_{\text{hetero}}} = \frac{[\text{M} \cdot \text{ref} \cdot \text{A}_R]^+ / [\text{M} \cdot (\text{ref})_2]^+}{[\text{M} \cdot \text{ref} \cdot \text{A}_S]^+ / [\text{M} \cdot (\text{ref})_2]^+} \quad (2)$$

relative stability of the “homo” versus the “hetero”  $[\text{M} \cdot \text{ref} \cdot \text{A}]^+$  cluster ion ( $\Delta\Delta G$ ) is calculated from Equation (3), where  $T_{\text{eff}}$  is the effective temperature<sup>[18]</sup> and  $R$  is the gas constant.

$$\ln R_{\text{chiral}} = \frac{\Delta\Delta G}{RT_{\text{eff}}} \quad (3)$$

We describe here the application of the kinetic method of Cooks and co-workers to the enantiodiscrimination of

*O*-phosphoserine (<sup>OP</sup>Ser). The study is intended to demonstrate the sensitivity and the reproducibility of the method and its potential in quantifying the enantiomeric excess of <sup>OP</sup>Ser in biological specimens.

Singly charged trimeric clusters  $[\text{M} \cdot (\text{ref})_2 \cdot \text{A}]^+$  ( $\text{M} = \text{H}, \text{Na}$ ) were generated by electrospraying aqueous methanol solutions containing a pure enantiomer of <sup>OP</sup>Ser and a chiral reference compound, namely, (*R*)-(-)- ( $E_R$ ), (*S*)-(+)- (1-aminoethyl)phosphonic acid ( $E_S$ ), or *O*-phospho-L-threonine (<sup>OP</sup>Thr<sub>L</sub>). The use

of these reference compounds with size and functionality similar to those of the <sup>OP</sup>Ser analyte is dictated by the desirability to minimize entropy effects on  $[\text{M} \cdot (\text{ref})_2 \cdot \text{A}]^+$  fragmentation.<sup>[19]</sup> The CID of the selected trimeric cluster ions  $[\text{M} \cdot (\text{ref})_2 \cdot \text{A}]^+$  ( $\text{M} = \text{H}, \text{Na}$ ) was carried out in a triple-quadrupole mass spectrometer (QqQ). For comparative purposes, the CID spectra of both the homochiral  $[\text{Na} \cdot (\text{OPThr}_L)_2 \cdot \text{OPSer}_L]^+$  and the heterochiral  $[\text{Na} \cdot (\text{OPThr}_L)_2 \cdot \text{OPSer}_D]^+$  ions were further investigated with a Fourier-transform ion cyclotron resonance (FT-ICR) mass spectrometer.

The lower part of Figure 2 shows the QqQ-CID spectra of these latter species measured at a collision energy of 10 eV (lab frame). The FT-ICR-SORI-CID spectra (SORI = sustained off-resonance irradiation) of the same species are illustrated in the upper part of Figure 2. The closeness of the calculated  $R_{\text{chiral}}$  factors (0.67 (QqQ) and 0.69 (FT-ICR)) points to the methodology having a negligible effect on the enantiodiscrimination of the analyte. The  $R_{\text{chiral}}$  values show

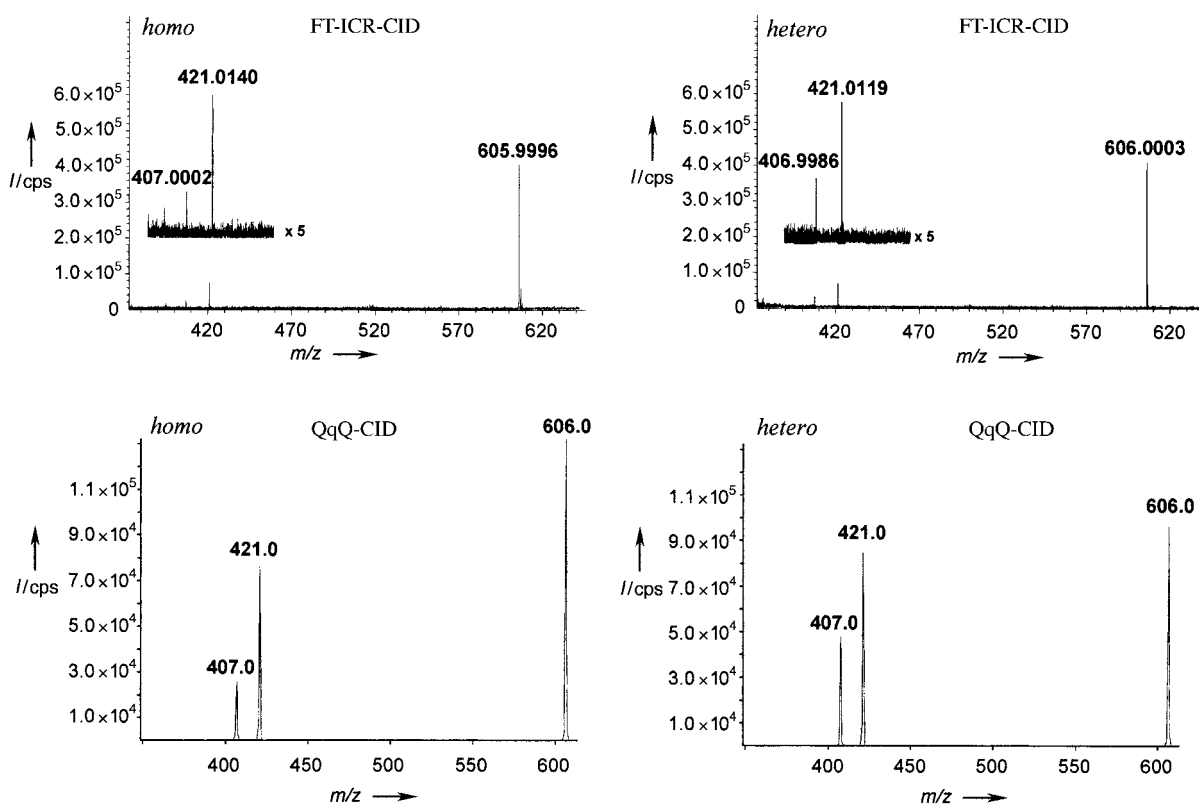


Figure 2. Top: SORI-CID spectra of  $[\text{Na} \cdot (\text{OPThr}_L)_2 \cdot \text{OPSer}_L]^+$  (*homo*) and  $[\text{Na} \cdot (\text{OPThr}_L)_2 \cdot \text{OPSer}_D]^+$  (*hetero*), obtained by FT-ICR mass spectrometry ( $m/z$ : 606 ( $[\text{Na} \cdot (\text{OPThr}_L)_2 \cdot \text{OPSer}]^+$ ), 421 ( $[\text{Na} \cdot (\text{OPThr}_L)_2]^+$ ), 407 ( $[\text{Na} \cdot \text{OPThr}_L \cdot \text{OPSer}]^+$ )). Bottom: CID-MS<sup>2</sup> spectra of  $[\text{Na} \cdot (\text{OPThr}_L)_2 \cdot \text{OPSer}_L]^+$  (*homo*) and  $[\text{Na} \cdot (\text{OPThr}_L)_2 \cdot \text{OPSer}_D]^+$  (*hetero*), using a triple quadrupole (QqQ; collision energy 10 eV; lab frame).

the homochiral  $[\text{Na} \cdot {}^{\text{OP}}\text{Thr}_L \cdot {}^{\text{OP}}\text{Ser}_L]^+$  fragment has a lower stability than the heterochiral  $[\text{Na} \cdot {}^{\text{OP}}\text{Thr}_L \cdot {}^{\text{OP}}\text{Ser}_D]^+$  one.

The results obtained from the QqQ-CID experiments on the homochiral  $[\text{H} \cdot (\text{E}_S)_2 \cdot {}^{\text{OP}}\text{Ser}_L]^+$  and the heterochiral  $[\text{H} \cdot (\text{E}_S)_2 \cdot {}^{\text{OP}}\text{Ser}_D]^+$  clusters as a function of the collision energy (6–10 eV (lab frame)) are summarized in Table 1. It should be noted that while both the  $R_{\text{hom}}/R_{\text{hetero}}$  and  $R'_{\text{hom}}/R'_{\text{hetero}}$  terms from the CID of  $[\text{H} \cdot (\text{E}_S)_2 \cdot {}^{\text{OP}}\text{Ser}_L]^+$  tend to decrease on increasing the collision energy from 6 to 10 eV, their  $R_{\text{chiral}} = R_{\text{hom}}/R_{\text{hetero}}$  ratios are scattered around the average value of  $0.84 \pm 0.07$ . A similar average value ( $0.87 \pm 0.06$ ) is obtained for the  $R'_{\text{hom}}/R'_{\text{hetero}}$  ratios from the CID of  $[\text{H} \cdot (\text{E}_R)_2 \cdot {}^{\text{OP}}\text{Ser}_L]^+$ . The remarkable reproducibility of the measurements is further testified by the average  $R_{\text{hom}}/R_{\text{hetero}}$  and  $R'_{\text{hom}}/R'_{\text{hetero}}$  ratios (last two columns of Table 1), which are found to coincide with the  $R_{\text{hom}}/R_{\text{hetero}}$  and  $R'_{\text{hom}}/R'_{\text{hetero}}$  ratios within their combined experimental uncertainties.

The QqQ-CID spectra of the trimeric complexes  $[\text{Na} \cdot (\text{E}_S)_2 \cdot {}^{\text{OP}}\text{Ser}_L]^+$  and  $[\text{Na} \cdot (\text{E}_S)_2 \cdot {}^{\text{OP}}\text{Ser}_D]^+$  display features which prevent any quantitative evaluation of  ${}^{\text{OP}}\text{Ser}_L$  versus  ${}^{\text{OP}}\text{Ser}_D$  discrimination. Indeed, the fragmentation patterns of both diastereomers are characterized by the presence of a minor signal corresponding to the loss of two  $\text{E}_S$  molecules. Their abundance increases from about 7% (7 eV) to about 11% (12 eV) of the total ion current. Since it is not possible to assign firmly the origin of this fragment to a given precursor, either from  $[\text{Na} \cdot \text{E}_S \cdot {}^{\text{OP}}\text{Ser}]^+$  after the loss of a first  $\text{E}_S$  molecule or directly from  $[\text{Na} \cdot (\text{E}_S)_2 \cdot {}^{\text{OP}}\text{Ser}]^+$ , the corresponding  $R_{\text{chiral}}$  value could be affected by a systematic error. Such a drawback is absent in the fragmentation of the homochiral  $[\text{Na} \cdot (\text{OPSer}_L)_2 \cdot \text{E}_S]^+$  and the heterochiral  $[\text{Na} \cdot (\text{OPSer}_L)_2 \cdot \text{E}_R]^+$  clusters. Their fragmentation patterns as a function of the collision energy (7–12 eV) are illustrated in Table 2. The  $R_{\text{chiral}} = R_{\text{hom}}/R_{\text{hetero}}$  terms from the CID of  $[\text{Na} \cdot (\text{OPSer}_L)_2 \cdot \text{E}]^+$  converge around the average value of  $0.64 \pm 0.14$ . A similar average value ( $0.74 \pm 0.04$ ) is measured for the  $R'_{\text{hom}}/R'_{\text{hetero}}$  ratios from the fragmentation patterns of the diaster-

eomeric  $[\text{Na} \cdot (\text{OPSer}_D)_2 \cdot \text{E}_R]^+$  and  $[\text{Na} \cdot (\text{OPSer}_D)_2 \cdot \text{E}_S]^+$  cluster ions. Even in this case, the average  $R_{\text{hom}}/R'_{\text{hetero}}$  and  $R'_{\text{hom}}/R_{\text{hetero}}$  ratios (last two columns of Table 2) are found to coincide with the relevant  $R_{\text{hom}}/R_{\text{hetero}}$  and  $R'_{\text{hom}}/R'_{\text{hetero}}$  values within their combined experimental uncertainties.

A similar approach has been used to quantify  ${}^{\text{OP}}\text{Ser}$  enantiodiscrimination through the fragmentation spectra of their trimeric clusters with *O*-phospho-L-threonine ( $[\text{M} \cdot (\text{OPThr}_L)_2 \cdot {}^{\text{OP}}\text{Ser}]^+$ ; with  $\text{M} = \text{H}$  or  $\text{Na}$ ). The relevant results, combined with those from Tables 1 and 2, are summarized in Table 3. These values provide a measure of the reliability and the reproducibility of the MS<sup>2</sup> approach. The chiral selectivity factors can be further evaluated in terms of the underlying thermochemistry by using Equation (3). The difference be-

Table 3. Degree of chiral recognition of *O*-phosphoserine.

| M  | ref                          | Chiral selectivity factor            | $\Delta\Delta G$ (KJ mol <sup>-1</sup> ) |
|----|------------------------------|--------------------------------------|--|
| H  | $\text{E}_S$                 | $R_{\text{chiral}} = 0.84 \pm 0.07$  | $-1.4 \pm 0.7$                           |
| H  | $\text{E}_R$                 | $R'_{\text{chiral}} = 0.87 \pm 0.06$ | $-1.1 \pm 0.6$                           |
| H  | ${}^{\text{OP}}\text{Thr}_L$ | $R_{\text{chiral}} = 0.88 \pm 0.11$  | $-1.0 \pm 0.9$                           |
| Na | $\text{E}_S$                 | $R'_{\text{chiral}} = 0.65 \pm 0.08$ | $-3.4 \pm 0.9$                           |
| Na | $\text{E}_R$                 | $R'_{\text{chiral}} = 0.67 \pm 0.08$ | $-3.2 \pm 0.9$                           |
| Na | ${}^{\text{OP}}\text{Thr}_L$ | $R_{\text{chiral}} = 0.75 \pm 0.12$  | $-2.3 \pm 1.2$                           |

tween the change in free energy  $\Delta\Delta G$  reflects the different attractive electrostatic and repulsive steric interactions operating in the diastereomeric  $[\text{M} \cdot \text{ref} \cdot \text{A}]^+$  clusters, whose effective temperature  $T_{\text{eff}}$  is estimated as approximately 950 K from previous studies on strictly related systems.<sup>[20]</sup> The negative  $\Delta\Delta G$  values indicate that the heterochiral complexes are more stable than the homochiral analogues. Their stability difference is larger for the Na-bound complexes than for the proton-bound ones.<sup>[21]</sup>

Although the chiral selectivity values of Table 3 are not particularly large,<sup>[22]</sup> the accuracy and sensitivity of the MS<sup>2</sup> approach can nevertheless be used for quantifying the optical

Table 1. Fragment-ion abundance ratios  $[\text{H} \cdot \text{ref} \cdot \text{A}]^+ / [\text{H} \cdot (\text{ref})_2]^+$  from CID of diastereomeric  $[\text{H} \cdot (\text{ref})_2 \cdot \text{A}]^+$  complexes at various collision energies (lab frame).

| Collision energy [eV] | ref          | A = ${}^{\text{OP}}\text{Ser}_L$<br>$R_{\text{hom}}$ | A = ${}^{\text{OP}}\text{Ser}_D$<br>$R_{\text{hetero}}$ | $R_{\text{chiral}}$<br>( $R_{\text{hom}}/R_{\text{hetero}}$ ) | ref          | A = ${}^{\text{OP}}\text{Ser}_D$<br>$R'_{\text{hom}}$ | A = ${}^{\text{OP}}\text{Ser}_L$<br>$R'_{\text{hetero}}$ | $R'_{\text{chiral}}$<br>( $R'_{\text{hom}}/R'_{\text{hetero}}$ ) | $R''_{\text{chiral}}$<br>( $R_{\text{hom}}/R'_{\text{hetero}}$ ) | $R'''_{\text{chiral}}$<br>( $R'_{\text{hom}}/R_{\text{hetero}}$ ) |
|-----------------------|--------------|--|---|---|--------------|---|--|--|--|---|
| 6                     | $\text{E}_S$ | 2.36   | 2.92  | 0.81  | $\text{E}_R$ | 2.21  | 2.45   | 0.90   | 0.96   | 0.76  |
| 7                     | $\text{E}_S$ | 2.12   | 2.63  | 0.81  | $\text{E}_R$ | 2.17  | 2.35   | 0.92   | 0.90   | 0.83  |
| 8                     | $\text{E}_S$ | 1.97   | 2.40  | 0.82  | $\text{E}_R$ | 1.70  | 2.06   | 0.82   | 0.96   | 0.71  |
| 9                     | $\text{E}_S$ | 1.84   | 2.02  | 0.91  | $\text{E}_R$ | 1.69  | 2.08   | 0.81   | 0.88   | 0.84  |
| 10                    | $\text{E}_S$ | 1.78   | 2.04  | 0.87  | $\text{E}_R$ | 1.76  | 1.91   | 0.92   | 0.93   | 0.86  |
|                       |              |  |   | Av: $0.84 \pm 0.07$   |              |   |  |  | Av: $0.87 \pm 0.06$  | Av: $0.93 \pm 0.05$   |
|                       |              |  |   |   |              |   |  |  | Av: $0.80 \pm 0.09$  |   |

Table 2. Fragment-ion abundance ratios  $[\text{Na} \cdot \text{ref} \cdot \text{A}]^+ / [\text{Na} \cdot (\text{ref})_2]^+$  from CID of diastereomeric  $[\text{Na} \cdot (\text{ref})_2 \cdot \text{A}]^+$  complexes at various collision energies (lab frame).

| Collision energy [eV] | ref                          | A = $\text{E}_S$<br>$R_{\text{hom}}$ | A = $\text{E}_R$<br>$R_{\text{hetero}}$ | $R_{\text{chiral}}$<br>( $R_{\text{hom}}/R_{\text{hetero}}$ ) | ref                          | A = $\text{E}_R$<br>$R'_{\text{hom}}$ | A = $\text{E}_S$<br>$R'_{\text{hetero}}$ | $R'_{\text{chiral}}$<br>( $R'_{\text{hom}}/R'_{\text{hetero}}$ ) | $R''_{\text{chiral}}$<br>( $R_{\text{hom}}/R'_{\text{hetero}}$ ) | $R'''_{\text{chiral}}$<br>( $R'_{\text{hom}}/R_{\text{hetero}}$ ) |
|-----------------------|------------------------------|--------------------------------------|---|---|------------------------------|---------------------------------------|--|--|--|---|
| 7                     | ${}^{\text{OP}}\text{Ser}_L$ | 0.17                                 | 0.34                                    | 0.50  | ${}^{\text{OP}}\text{Ser}_D$ | 0.20                                  | 0.30                                     | 0.67   | 0.57   | 0.59  |
| 8                     | ${}^{\text{OP}}\text{Ser}_L$ | 0.19                                 | 0.28                                    | 0.68  | ${}^{\text{OP}}\text{Ser}_D$ | 0.21                                  | 0.26                                     | 0.81   | 0.73   | 0.75  |
| 9                     | ${}^{\text{OP}}\text{Ser}_L$ | 0.23                                 | 0.40                                    | 0.57  | ${}^{\text{OP}}\text{Ser}_D$ | 0.27                                  | 0.36                                     | 0.75   | 0.64   | 0.67  |
| 10                    | ${}^{\text{OP}}\text{Ser}_L$ | 0.19                                 | 0.28                                    | 0.68  |                              |                                       |  |  |  |   |
| 11                    | ${}^{\text{OP}}\text{Ser}_L$ | 0.21                                 | 0.32                                    | 0.65  |                              |                                       |  |  |  |   |
| 12                    | ${}^{\text{OP}}\text{Ser}_L$ | 0.23                                 | 0.31                                    | 0.74  |                              |                                       |  |  |  |   |
|                       |                              |                                      |   | Av: $0.64 \pm 0.14$   |                              |                                       |  |  | Av: $0.74 \pm 0.07$  | Av: $0.65 \pm 0.08$   |
|                       |                              |                                      |   |   |                              |                                       |  |  | Av: $0.67 \pm 0.08$  |   |

purity of  $^{OP}Ser$ . A calibration curve can be derived from the analysis of the QqQ-CID spectra of trimeric  $[Na \cdot (^{OP}Thr_L)_2 \cdot ^{OP}Ser]^+$  complexes containing variable  $^{OP}Ser_L$  versus  $^{OP}Ser_D$  proportions. The results show a linear relationship of  $\ln([Na \cdot ^{OP}Thr_L \cdot ^{OP}Ser]^+ / [Na \cdot (^{OP}Thr_L)_2]^+)$  versus the molar fraction of the D enantiomer of  $^{OP}Ser$  ( $\% ^{OP}Ser_D$ ; Figure 3).

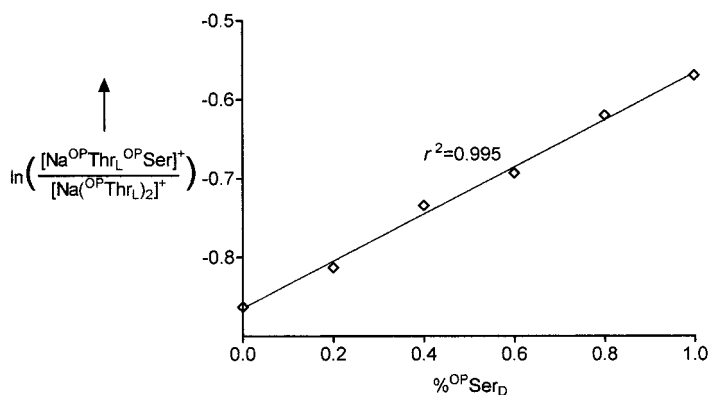


Figure 3. Calibration curve for the chiral analysis of *O*-phosphoserine.

The present study highlights several successful applications of the kinetic method of Cooks and co-workers to the enantiodiscrimination of chiral compounds. The studies demonstrate that the kinetic method is sufficiently precise and accurate to be potentially applicable for quantifying the enantiomeric excess of *O*-phosphoserine in proteomic analysis. The ESI-MS<sup>2</sup> procedure is fast and does not rely on any manipulation of the sample. The chiral selectivity factors also do not seem to depend upon the specific instrumentation used (FT-ICR or QqQ). Given the extremely high resolution normally attainable in FT-ICR experiments (full width at half height (FWHH) > 50000), the FT-ICR-SORI-CID procedure appears particularly suitable for the routine analysis of chiral *O*-phosphoserine and -threonine even in complex biological matrices. Extension of this work to other phosphorylated amino acids is in progress.

### Experimental Section

**ESI-MS<sup>2</sup> experiments:** The CID experiments were performed by using both a commercial API 100/300 triple-quadrupole (QqQ) mass spectrometer from Perkin Elmer Sciex Instruments and a commercial APEX 47e FT-ICR mass spectrometer from Bruker Spectrospin. Both instruments were equipped with an ESI source and a syringe pump. Operating conditions for the ESI source: spray voltage: 3.8 kV, capillary temperature: 298 K, sheath gas (N<sub>2</sub>) flow rate: 30 units (roughly 0.75 L min<sup>-1</sup>). The selected gas-phase complexes were generated by electrospraying at a flow rate of 10 μL min<sup>-1</sup> solutions of water/methanol (50/50) containing equimolar amounts (10 μM each) of the optically pure *O*-phosphoserine and a chiral reference compound, that is, (*R*)-(-)-(1-aminoethyl)phosphonic acid, its *S* enantiomer, or *O*-phospho-L-threonine. The CID experiments on the so-formed diastereomeric complexes were conducted in the positive-ion mode.

**QqQ-CID experiments:** In the full-scan QqQ-MS<sup>2</sup> mode, the diastereomeric cluster ions were isolated in the first mass-analyzing quadrupole *Q*, excited in the second “rf-only” quadrupole *q* by collision with N<sub>2</sub> (pressure around 10 mbar, energy range 6–12 eV in the laboratory frame), and eventually analyzed in the third quadrupole *Q* of the instrument.

**FT-ICR-CID experiments:** In the FT-ICR-MS<sup>2</sup> mode, the same cluster ions were injected from the external source of the instrument into the analyzer, quenched by multiple collision with N<sub>2</sub>, admitted into the analyzer through

a pulsed valve assembly (the nominal peak pressure was approximately 5 × 10<sup>-6</sup> mbar), and eventually isolated by broad-band ejection of the unwanted fragments. SORI-CID experiments were carried out by accelerating the quenched ions with an activation frequency 0.25 kHz higher than the cyclotron frequency of the ion, and by allowing them to collide for 2 s with the N<sub>2</sub> present in the analyzer at a constant pressure of 2 × 10<sup>-8</sup> mbar.

Received: April 24, 2001  
Revised: August 1, 2001 [Z16990]

- [1] P. Cohen, *Trends Biochem. Sci.* **1992**, *17*, 408.
- [2] T. Hunter, *Methods Enzymol.* **1991**, *200*, 3.
- [3] M. J. Hubbard, P. Cohen, *Trends Biochem. Sci.* **1993**, *18*, 172.
- [4] T. Hunter, B. Sefton, *Proc. Natl. Acad. Sci. USA* **1980**, *77*, 1311.
- [5] L. Gorbics, L. Urge, E. Lang, G. I. Szendrel, L. Otvos, Jr., *J. Liq. Chromatogr.* **1994**, *17*, 175.
- [6] E. Neufeld, J. H. Goren, D. Boland, *Anal. Biochem.* **1989**, *177*, 138.
- [7] M. Brauer, B. D. Skykes, *Methods Enzymol.* **1984**, *107*, 37.
- [8] R. Hoffman, O. Reichert, W. O. Wachs, M. Zeppezauer, H. R. Kalbizer, *Int. J. Pept. Protein Res.* **1994**, *35*, 161.
- [9] J. D. Harrison, *Protein Phosphorylation—A Practical Approach* (Ed.: D. G. Hardie), Oxford University Press, Oxford, **1992**, p. 22.
- [10] S. A. Carr, M. E. Hemling, M. F. Bean, G. D. Roberts, *Anal. Chem.* **1991**, *63*, 2802.
- [11] R. Aebersold, D. R. Goodlett, *Chem. Rev.* **2001**, *101*, 269, and references therein.
- [12] A. Filippi, A. Giardini, S. Piccirillo, M. Speranza, *Int. J. Mass Spectrom.* **2000**, *198*, 137, and references therein.
- [13] W. A. Tao, D. Zhang, E. N. Nikolaev, R. G. Cooks, *J. Am. Chem. Soc.* **2000**, *122*, 10598.
- [14] W. A. Tao, R. G. Cooks, *Angew. Chem.* **2001**, *113*, 779; *Angew. Chem. Int. Ed.* **2001**, *40*, 757.
- [15] G. Gregorean, J. Ramirez, S. H. Ahn, C. B. Lebrilla, *Anal. Chem.* **2000**, *72*, 4275.
- [16] W. Y. Shen, P. S. H. Wong, R. G. Cooks, *Rapid Commun. Mass Spectrom.* **1997**, *11*, 71.
- [17] K. Vekey, G. Czira, *Anal. Chem.* **1997**, *69*, 1700.
- [18] J. Laskin, J. H. Futrell, *J. Phys. Chem.* **2000**, *104*, 8829.
- [19] R. G. Cooks, J. S. Patrick, T. Kotiaho, S. A. McLuckey, *Mass Spectrom. Rev.* **1994**, *13*, 287.
- [20] A. Paladini, C. Calcagni, M. Satta, T. Di Palma, M. Speranza, A. Laganà, G. Fago, A. Filippi, A. Giardini-Guidoni, *Chirality* **2001**, in press.
- [21] The different stability of the diastereomeric complexes  $[M \cdot ^{OP}Thr_L \cdot ^{OP}Ser]^+$  ( $M = H$  or  $Na$ ) suggests that the ESI-MS<sup>2</sup> approach can be conveniently employed to enantiodiscriminate  $^{OP}Thr$  by using enantiomerically pure  $^{OP}Ser$  as the reference.
- [22] Previous studies on  $\alpha$ -hydroxy acids (W. A. Tao, L. Wu, R. G. Cooks, *Chem. Commun.* **2000**, 2023) show that precise chiral quantitation is still achievable, even with low selectivity values.